VOL. 11, NO. 12, JUNE 2016 ISSN 1819-6608
ARPN Journal of Engineering and Applied Sciences

www.arpnjournals.com

TEXTILE DIAMOND DIPOLES FOR BODY CENTRIC COMMUNICATIONS AT 2.45GHZ AND 5.8GHZ

Kamilia Kamardin[1], Mohamad Kamal A. Rahim[2], Noor Asmawati Samsuri[2], Mohd Ezwan Jalil[2], Salwani Mohd Daud[1], Suriani Mohd Sam[1] and Noor Azurati Ahmad[1]
[1]Computer Systems Engineering Group, Advanced Informatics School, Universiti Teknologi Malaysia, Kuala Lumpur, Malaysia
[2]Department of Communication Engineering, Faculty of Electrical Engineering, Universiti Teknologi Malaysia, Johor Bahru, Malaysia
E-Mail: kamilia@utm.my

ABSTRACT

This study proposes textile diamond dipoles for body centric communication that operate at 2.45GHz and 5.8GHz. The proposed antennas have been rigorously tested under wearable and body centric measurements. Both substrates and conducting parts of the diamond dipoles are entirely made of textiles; which is deemed fit for wearable communications. Experiments such as bending, wetness and SAR were performed to investigate the antennas' performance for body communication realization. Bending was found not to cause any significant performance disruption. On the other hand, since the proposed antenna is not made of water-proof material, the performance was distorted under wet condition. However, once the antenna was dried out, the original performance was achieved. SAR measurement was also conducted and significant SAR values were observed when placing the proposed diamond dipoles close to human body.

Keywords: textile antenna, diamond dipole, wearable antenna, bending, wetness, specific absorption rate.

INTRODUCTION

Wearable technology is on the verge of tremendous growth following the introduction of wireless body centric communication. Due to the rapid development of wireless communications, demand for new antenna technologies will increase dramatically for the next coming years. This phenomenon indicates a strong potential for wired-communication network to be replaced in the future where antenna will play an important role.

It can be imagined that in the future, clothing may have a number of electronics built into them. Due to this, there is a demand for flexible fabric antenna that can be easily attached to clothing. These antennas are becoming more flexible and lightweight, and soon a wide range of unobtrusive wearable and ubiquitous computing equipment will be integrated into our personal everyday wear, in health care, military, sports, space applications and many more [1].

The research on wearable antennas has attracted vast interest amongst researchers in the recent years. They have been applied in medical, biotelemetry, telemedicine, military, wireless power transmission, and in many other industries. The earliest study on wearable antenna was published in 1999 by Salonen *et al*. [2] that proposed a dual-band planar inverted-F antenna constructed using printed circuit board technology. Since then, research on wearable antennas has been blooming amongst antenna researchers including works on non-textile antennas (i.e. no-fabric) as well as textile antennas. Wearable non-textile antennas are proposed in the form of printed circuit board [3], flexible material [4] and foam [5].

Wearable antennas made of textile are the most comfortable, thus this type of antenna is proposed in this study. The development of textile diamond dipoles that operates at 2.45GHz and 5.8GHz is presented in this work. The proposed antenna will be tested under rigorous wearable and body centric communication to explore its viability for body centric applications.

Textile diamond dipole

Compared to conventional dipole, diamond dipole offers wider bandwidth. Two diamond dipoles are designed to operate at 2.45GHz and 5.8GHz respectively. Initially, the estimated parameters are calculated based on theoretical formulae. Diamond dipole originates from inverted bow tie dipole. Therefore, similar equations used to design bow tie antenna is applied [6]. These equations serve as design guideline for the simulation. The calculated horizontal lengths of the radiating element, L1 are 61mm and 25.6mm for 2.45GHz and 5.8GHz antennas respectively. Series of simulations using CST Microwave Studio have been conducted in order to obtain optimum configuration. Figure-1 and Figure-2 show the 2.45GHz and 5.8GHz textile diamond dipoles design layout along with its optimized dimensions respectively. The substrate of the dipoles are made of fleece fabric.

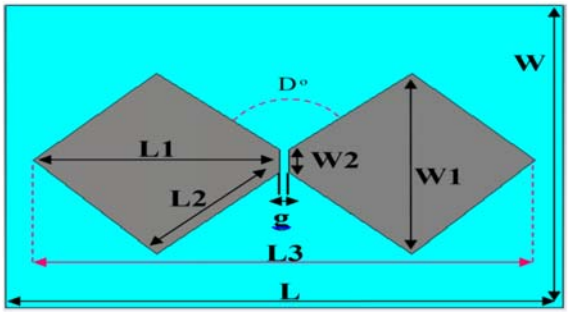

Figure-1. 2.45GHz textile diamond dipole with its dimensions in mm. L=60, W=45, L1=26.5, L2=18, W1=27, W2=3.4, g=1.

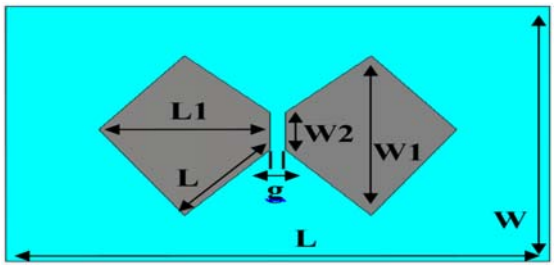

Figure-2. 5.8GHz textile diamond dipole with its dimensions in mm. L=35, W=23, L1=11, L2=8, W1=14.4, W2=3.4, g=1.

Subsequent to the simulation process, fabrication of the antennas follows. The prototypes of the two diamond dipoles are shown in Figure-3. Pigtail SMA has been used as the connector for both of the diamond dipoles. To validate the simulation findings, measurements are performed. Figure-4 plots the comparison between simulated and measured S_{11} for both diamond dipoles. Figure-4(a) presents the return loss of 2.45GHz diamond dipole whilst the S_{11} for 5.8GHz diamond dipole is shown in Figure-4(b). Both results show reasonable agreement between simulations and measurements.

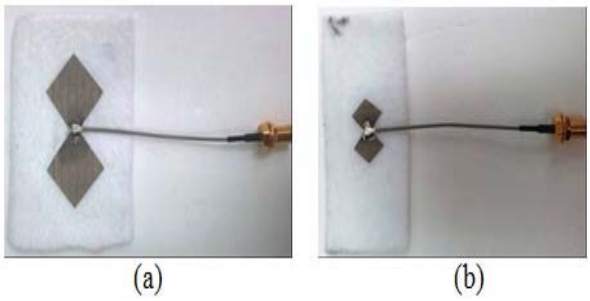

Figure-3. Fabricated textile diamond dipoles (a) 2.45GHz (b) 5.8GHz.

The measured S_{11} for 2.45GHz diamond dipole has a return loss depth of -33.64dB, and -15.39dB for the 5.8GHz diamond dipole. The measured bandwidth for 2.45GHz dipole is found to be 750MHz of 30.93% from 2.05GHz to 2.8GHz. On the other hand, 5.8GHz diamond dipole has a measured bandwidth of 1.44GHz (24.74%) that ranging from 5.1GHz to 6.54GHz. Results in Figure-4 show minor differences between simulated and measured S11 for both 2.45GHz and 5.8GHz textile diamond dipoles. It is noticed that the measured return loss for both dipoles are higher that the simulated results. The non-uniformity between the fabricated prototype and simulated structure is expected to cause the discrepancies between simulated and measured results. To reduce simulation size and time, the pigtail SMA connector is not included in the simulated structure. As a replacement, discrete port has been used to excite the antenna in the simulation.

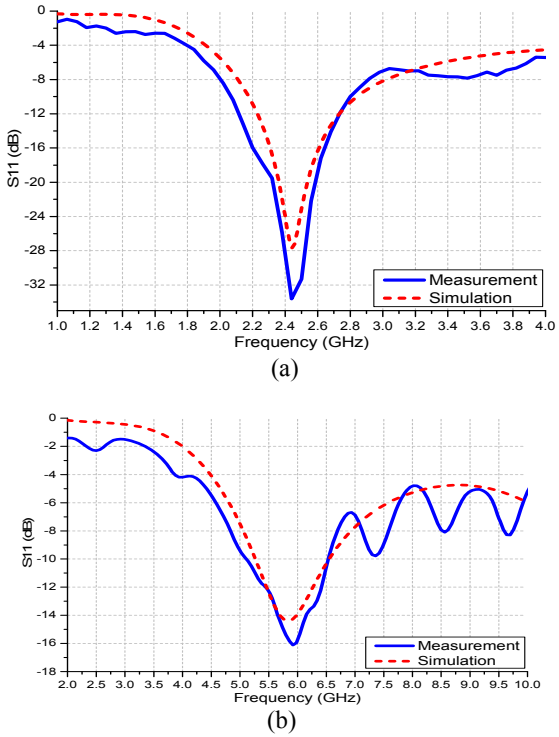

Figure-4. Measured and simulated S_{11} of textile diamond dipoles (a) 2.45GHz (b) 5.8GHz.

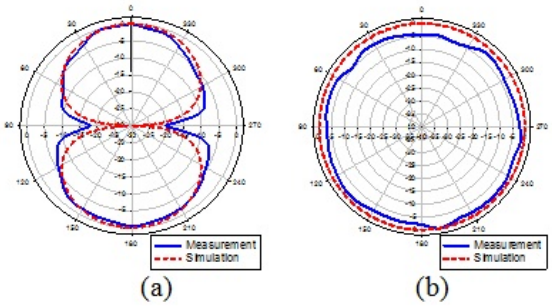

Figure-5. Measured and simulated radiation patterns of 2.45GHz diamond dipole at resonant frequency (a) E plane (b) H plane.

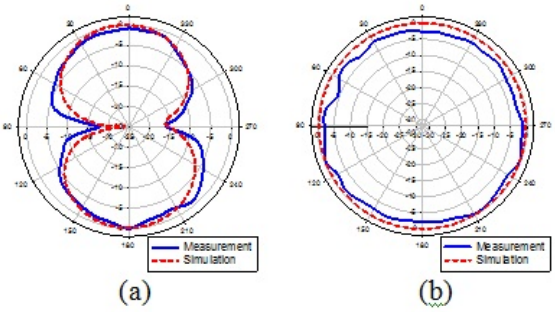

Figure-6. Measured and simulated radiation patterns of 5.8GHz diamond dipole at 5.8GHz (a) E plane (b) H plane.

Table-1. Students name list.

	Frequency (GHz)	Bandwidth (GHz)	Gain (dB)
Simulation	**2.45**	2.17 – 2.84 (26.75%)	2.04
	5.8	5.26 – 6.55 (21.85%)	2.13
Measurement	**2.45**	2.05 – 2.8 (30.93%)	3.09
	5.8	5.1 – 6.54 (24.74%)	3.17

The radiation patterns of both 2.45GHz and 5.8GHz diamond dipoles are measured in an anechoic chamber. Figure-5 and Figure-6. shows the comparison between simulated and measured patterns. Good agreement between measured and simulated patterns of the two antennas can be seen in both E and H planes. The measured gain for the 2.45GHz dipole is 3.09dB and the simulated gain is 2.04dB. The 5.8GHz dipole has a measured gain of 3.17dB and simulated gain of 2.13dB. Both diamond dipoles have simulated efficiencies of 98.77% and 95.14% for 2.45GHz and 5.8GHz dipoles respectively. Table 1 tabulates the measured and simulated bandwidth and gain of both 2.45GHz and 5.8GHz diamond dipoles. The discrepancies between simulated and measured gain is predicted due to the dissimilarity between the materials used in the simulation and measurement.

WEARABLE AND BODY CENTRIC MEASUREMENTS

Bending

The performance of antenna under bending condition is an important factor to look into for body centric communication. Wearable antenna is exposed to the change of human body's movements and posture, hence the antenna is prone to bending. Polystyrene cylinder that represents a human arm size with diameter of 80mm is used as the bending gauge. Such small cylinder is used to test the performance of the antenna under high bending exposure. In this study, the textile diamond dipoles are bent in horizontal orientation as shown in the Figure-7.

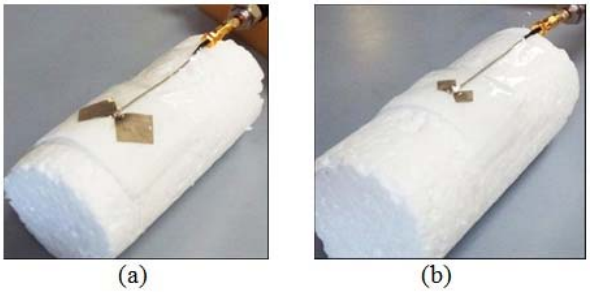

Figure-7. Bending measurement of textile diamond dipoles (a) 2.45GHz (b) 5.8GHz.

The measured return loss of bent 2.45GHz diamond dipole is shown in Figure-8. Comparing to the flat diamond dipole, reasonable agreement can be noticed. It is observed that the resonant frequency remains stable despite in bending position. It is found that the return loss depth for the bent diamond dipole reduces from -33.6dB to -29.6dB. In general, it is found that the 2.45GHz diamond dipole gives good performance of resonant frequency and impedance bandwidth under bending condition.

Figure-9 on the other hand illustrates the measured S_{11} of bent and flat 5.8GHz diamond dipole. Similarly, the return loss of the bent 5.8GHz diamond dipole exhibits good match with the flat antenna's result. Only a slight shift is observed in the resonant frequency, which is negligible. The measured resonant frequency of the bent antenna is 5.98GHz compared to 5.92GHz for the flat case.

The radiation patterns of the bent diamond dipoles are shown in Figure-10 and Figure-11 for 2.45GHz and 5.8GHz antennas respectively. For all cases, good agreement between flat and bent antennas' radiation patterns are observed. Dipole's radiation characteristics are maintained for both antennas in E and H planes. Nevertheless, the beamwidth are seen to be marginally broadened for both dipoles. The direction of the antenna has been widened with the introduction of the bending curvature that leads to the slight increase of beamwidth.

The measured gain of the bent 2.45GHz dipole is 2.63dB compared to 3.09dB for the flat dipole. On the other hand, the gain for 5.8GHz diamond dipole is 2.86dB and 3.17dB for bent and flat forms respectively. The measured gains for both antennas under bending are observed to experience small drop. The slight drop is due to the fact that the antennas have become less directional because of bending.

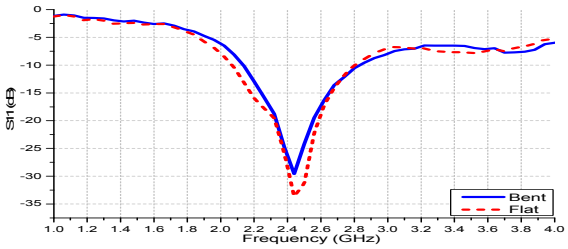

Figure-8. Measured S_{11} of 2.45GHz textile diamond dipole under bending condition.

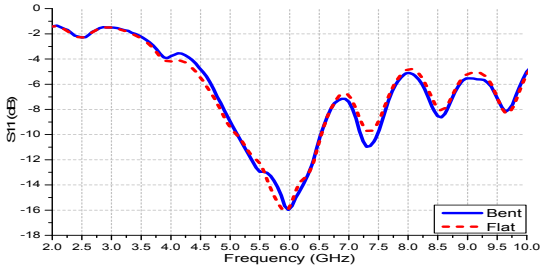

Figure-9. Measured S_{11} of 5.8GHz textile diamond dipole under bending condition.

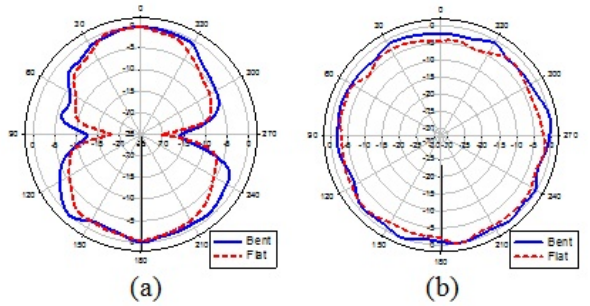

Figure-10. Measured radiation patterns of 2.45GHz textile diamond dipole under bending condition (a) E plane (b) H plane.

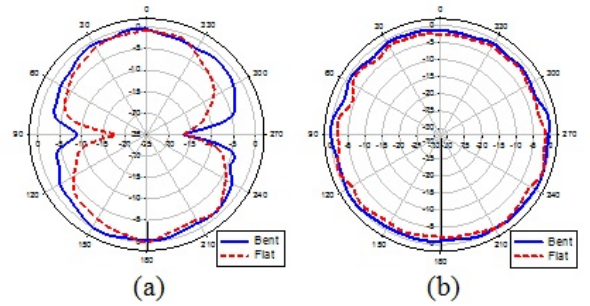

Figure-11. Measured radiation patterns of 5.8GHz textile diamond dipole under bending condition (a) E plane (b) H plane.

Wetness

Wearable antennas are exposed to sweat and rain hence there is possibility for the textile antennas to get wet. The standard fabric materials are not waterproof hence wetness measurement is essential. Wetness measurement in this study starts by immersing the textile antenna under water as shown in Figure-12. The antenna are soaked overnight for more than 12 hours. Then, the return loss of the antenna under complete wet state is measured as shown in Figure-12(b). The S_{11} of the wet antenna is immediately measured after being taken out from the water. Figure-13 shows the return loss comparison between different wetness conditions. Four different wetness conditions i.e. before washing, complete wet, damp and dry are compared. From the results, major distortion of S_{11} can be seen for the complete wet antenna. Water has high permittivity hence influencing the performance of the antenna. From the graph it can be observed that the resonant frequency is shifted to lower frequency due to high dielectric constant of the wet antenna. On the other hand, it can be seen that the return loss has returned close to the original S_{11} curve for the damp case. The damp dipole has a resonant frequency of 2.37GHz with return loss depth of -27.3dB. The damp antenna still has some moisture left in the substrate hence its dielectric constant is marginally higher than the original permittivity.

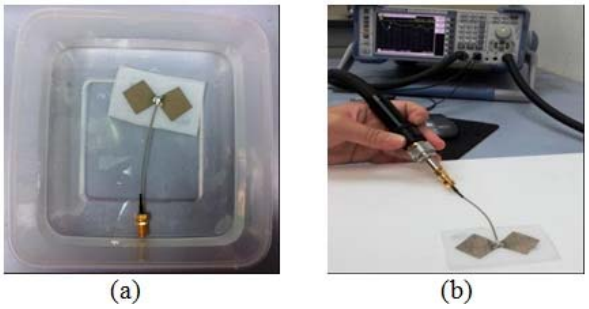

Figure-12. Wetness measurement for textile diamond dipole (a) antenna soaked in water (b) complete wet measurement.

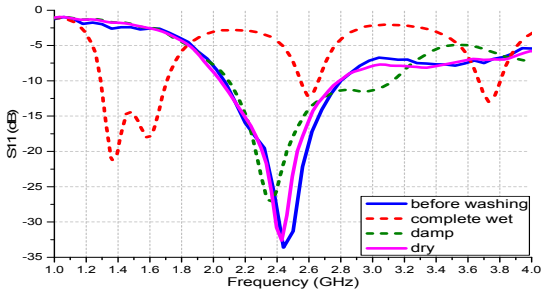

Figure-13. Measured S_{11} of textile diamond dipole under wet condition.

The pink curve denotes the fully dried S_{11} as shown in Figure-13. The fully dried dipole has resonant frequency of 2.43GHz with return loss depth of -32.6dB. There is a marginal difference between original and dry dipoles. The difference is predicted due to fabric shrinking that leads to the changes of antenna properties for the dry antenna. Nonetheless, good performance is still obtained by the fully dried antenna that is close to the original dipole's performance.

Specific absorption rate

Specific Absorption Rate (SAR) measurement is important since wearable antennas are meant to be placed very near to human body. The Federal Communications Commission (FCC) enforces a SAR limit of 1.6 W/kg for a mass of 1 gram while the limit enforced by International Commission on Non-Ionizing Radiation Protection (ICNIRP) is 2 W/kg for 10 grams of tissues. CST Microwave Studio is used to conduct SAR simulation. CST has Voxel family which consists of inhomogeneous biological models. In the simulation, the excitation used reference power of 1W. The SAR investigation was investigated at ISM 2.45GHz. The 3D SAR visualization is shown in Figure-14. The maximum SAR location is shown in the figure. As shown in the diagram, the maximum 3D 10g SAR value is 4.56 W/kg for textile diamond dipole. The computational peak SAR value for 1g human tissues is 9.29 W/kg.

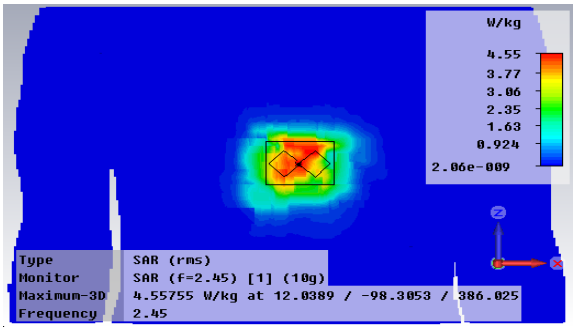

Figure-14. Simulated 3D maximum SAR visualization in CST

A simple system by Indexsar is used for the SAR measurement. The SAR measurement setup is shown in Figure-15. The setup includes Indexsar probe, its software and fibreglass phantom that represents human's torso part. For the measurement, the phantom body is filled with 2.45GHz equivalent homogeneous tissue stimulant liquid. The probe is immersed in the stimulant liquid for a number of distances. The probe will capture the measured data when antenna is excited to the phantom body. The data will be sent to the software that will calculate and display the peak point SAR value. The comparison between simulated and measured peak point SAR of the textile diamond dipole is shown in Figure-16. Results reveal the peak point SAR is 26.4 W/kg for simulation and 14.75 W/kg for measurement.

In addition, investigation on the separation distance between the antenna to the biological point in a human body is also carried. The antenna is positioned very near to the surface of human body. Then, the point SAR at different positions in the human body is captured at 0, 10, 20 and 50mm. 0 mm represents the closest point to the excitation while 50 mm is the furthest point inside the human body. The visual illustration of the arrangement is as shown in Figure-17. The results of peak point SAR values versus distance for both simulation and measurement is plotted in Figure-18. Results show that the trend between measured and simulated results yield good agreement. It can be observed that for both simulated and measured results, the peak point SAR values decreases as the distance increases.

Results show that good agreement in terms of trend between measured and simulated SAR has been obtained. However, there are differences of SAR amplitude between the measured and simulated values. The simulated point SAR values are observed to be higher that the measured values. The discrepancies is predicted caused by the outer shell of the fiberglass phantom used in the measurement. In the simulation, such outer dielectric shell is not included in the simulated structure where only biological voxel human model is simulated with the antenna. Due to this, high simulated SAR values is expected since the antenna excitation is very near to the human surface. In addition, small variation of distance between the antenna and human body in the simulation can lead to significant changes in the simulated SAR values. Furthermore, uncertainty is often associated with SAR measurement and therefore the difference between simulated and measured SAR amplitude normally happens.

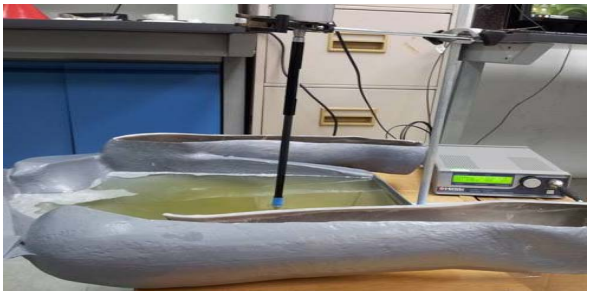

Figure-15. SAR measurement setup using Indexsar probe and tissue stimulant liquid with human phantom body made of fibre glass.

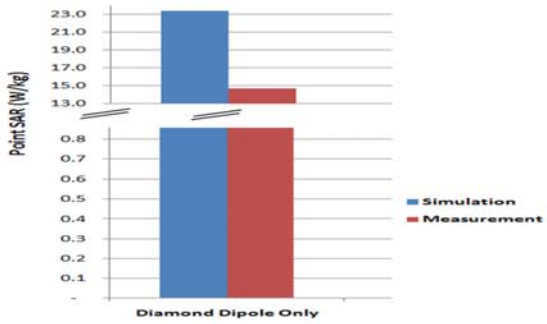

Figure-16. SAR comparison between simulated and measured results for diamond dipole antenna.

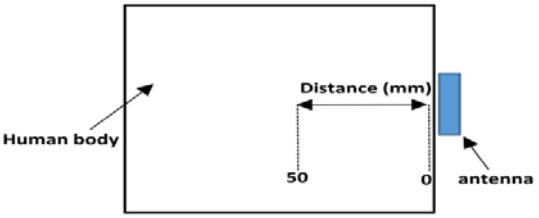

Figure-17. Visual illustration of the distance between antenna and human body.

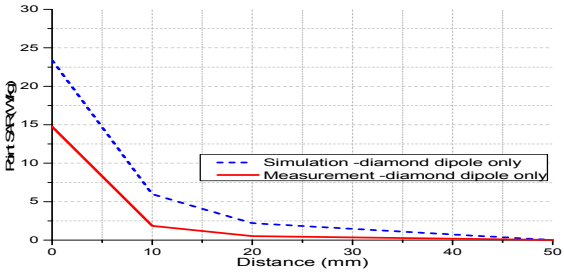

Figure-18. Simulated and measured peak point SAR versus distance for diamond dipole.

CONCLUSIONS

The development of textile diamond dipoles at 2.45GHz and 5.8GHz are presented in this paper. The antennas are designed, simulated, fabricated and measured. The antennas are also tested under wearable and body centric measurements. The bending, wetness and SAR effects on the proposed antennas have been explored thoroughly. Measured results show no significant effects on the performance of return loss, radiation pattern and gain are caused by bending. However, wetness measurement shows that completely wet antenna yields severe distortion of S_{11} performance. Nevertheless, the fully dried antenna yields performance that is close to the original before washing results. By using waterproof fabrics or plastic coating, wetness can be avoided. In addition, the proposed textile antenna are also tested under SAR measurement. Results show that significant concentration of SAR value is seen when the diamond dipole is placed on the human body. Artificial Magnetic Conductor (AMC) sheet is proposed to be placed between the antenna and human body to reduce the SAR value.

ACKNOWLEDGEMENTS

The authors wish to thank Malaysian Ministry of Higher Education (MOHE) and Universiti Teknologi Malaysia (UTM) for providing the Research Grant (Vote No: 02K02).

REFERENCES

[1] P. Salonen and H. Hurme. 2003. A Novel Fabric WLAN Antenna for Wearable Applications. IEEE International Symposium on Antennas and Propagation. pp. 700–703.

[2] P. Salonen, L. Sydanheimo, M. Keskilammi, and M. Kivikoski. 1999. A Small Planar Inverted-F Antenna for Wearable Applications. The Third Int. Symp. On Wearable Computers. pp. 95–100.

[3] C. Cibin, P. Leuchtmann, M. Gimersky, and R. Vahldieck. 2004. Modified E-Shaped Pifa Antenna for Wearable Systems. URSI Int. Symp. on Electromagnetic Theory. pp. 873–875.

[4] C. Cibin, P. Leuchtmann, M. Gimersky, R. Vahldieck, and S. Moscibroda. 2004. A Flexible Wearable Antenna. IEEE Int. Symp. on Antennas and Propag. pp. 3589–3592.

[5] C. Hertleer, H. Rogier, L. Vallozzi, and L. Van Langenhove. 2009. A Textile Antenna for Off-Body Communication Integrated Into Protective Clothing for Firefighters. IEEE Trans. Antennas Propag. 57(4): 919–925.

[6] W. S. Kaswiati and J. Suryana. 2012. Design and Realization of Planar Bow-Tie Dipole Array Antenna with Dual-Polarization at 2.4 GHz Frequency for Wi-Fi Access Point Application. 7th Int. Conf. on Telecom. Sys. Serv. and App. pp. 218–222.